

See discussions, stats, and author profiles for this publication at: <https://www.researchgate.net/publication/24243804>

# Organic Photodiodes for Biosensor Miniaturization

ARTICLE in ANALYTICAL CHEMISTRY · APRIL 2009

Impact Factor: 5.64 · DOI: 10.1021/ac8027323 · Source: PubMed

CITATIONS

32

READS

44

10 AUTHORS, INCLUDING:



**Lisa C Shriver-Lake**

United States Naval Research Laboratory

81 PUBLICATIONS 2,365 CITATIONS

SEE PROFILE



**Erwin Füreder**

Greiner Bio-One Diagnostics

4 PUBLICATIONS 141 CITATIONS

SEE PROFILE



**Christoph Winder**

TÜV Austria

34 PUBLICATIONS 2,812 CITATIONS

SEE PROFILE



**Max Sonnleitner**

Greiner Bio-One Diagnostics

27 PUBLICATIONS 709 CITATIONS

SEE PROFILE

# Organic Photodiodes for Biosensor Miniaturization

Jason R. Wojciechowski,<sup>†</sup> Lisa C. Shriver-Lake,<sup>†</sup> Mariko Y. Yamaguchi,<sup>†</sup> Erwin Füreder,<sup>‡</sup> Roland Pieler,<sup>‡</sup> Martin Schamesberger,<sup>‡</sup> Christoph Winder,<sup>‡</sup> Hans Jürgen Prall,<sup>‡</sup> Max Sonleitner,<sup>‡</sup> and Frances S. Ligler<sup>\*,†</sup>

Naval Research Laboratory, 4555 Overlook Avenue SW, Washington, D.C. 20375, and Nanoldent Technologies AG, Untere Donaulande 21-25, A-4020 Linz, Austria

Biosensors have successfully demonstrated the capability to detect multiple pathogens simultaneously at very low levels. Miniaturization of biosensors is essential for use in the field or at the point of care. While microfluidic systems reduce the footprint for biochemical processing devices and electronic components are continually becoming smaller, optical components suitable for integration—such as LEDs and CMOS chips—are generally still too expensive for disposable components. This paper describes the integration of polymer diodes onto a biosensor chip to create a disposable device that includes both the detector and the sensing surface coated with immobilized capture antibody. We performed a chemiluminescence immunoassay on the OPD substrate and measured the results using a hand-held reader attached to a laptop computer. The miniaturized biosensor with the disposable slide including the organic photodiode detected *Staphylococcal enterotoxin B* at concentrations as low as 0.5 ng/mL.

Next generation point-of-use testing requires compact systems that demonstrate a performance comparable to laboratory tests when operated by users without technical backgrounds. Future systems must be portable, automated, and sufficiently sensitive for the application. Ideally, measurements will be quantitative, and multiple targets will be detected simultaneously. Laboratory-on-a-chip (LOC) biosensors can be designed to satisfy these requirements.<sup>1</sup> Though the requirements are well-appreciated, the inclusion of LOC concepts into commercial biosensors has been slow, in particular because of limitations on the integration of optical and fluidic components.<sup>2</sup> While many current optical LOC biosensors employ microfluidics to miniaturize the sample processing and assay steps, external optical devices are typically used to interrogate the chip. Such external devices add substantial size, complexity, and cost to the detection system. Until detection is no longer accomplished via large, off-chip components such as PMTs, CCDs, and confocal scanners, a technology paradigm shift from the current “chip-in-a-lab” to a truly mobile “lab-on-a-chip” will not occur. Ideally, LOC optical detection systems will provide

rapid, sensitive, reliable results and employ readout instrumentation directly on a disposable chip.

A variety of optical readout methods are currently employed in biosensor technologies, including those based on fluorescence, chemiluminescence (CL), and absorption.<sup>3</sup> For LOC applications, chemiluminescence is an ideal detection method because of its inherent sensitivity and simplicity. In contrast to fluorescence-based sensors that require a light source to excite the sample, as well as detectors and emission filters, the only necessary components for chemiluminescence are detectors to measure the emitted photons generated during the CL reaction.<sup>4</sup> This reduced instrumentation requirement greatly decreases the cost and complexity of the detection system.

Potential detectors for optical sensors include CMOS chips, silicone photodiode arrays, and organic photodiodes. The optimal detection system must be small in size and located on-chip. Large, off-chip readout methods that require long working distances and include lenses often demonstrate high optical losses and decreased signal-to-noise ratios, rendering them unsuitable for many applications. CMOS chips<sup>5,6</sup> and silicon photodiode arrays<sup>7</sup> are capable of providing reasonable sensitivity for detection of low analyte concentrations but are too expensive and complicated to fabricate as an integral part of a disposable sensor.<sup>8,9</sup> Organic photodiodes (OPDs), in comparison, offer the best potential for future LOC technology, as they are inexpensive,<sup>10,11</sup> are easily fabricated, have a large dynamic range,<sup>9,12,13</sup> and are highly sensitive.<sup>4,12,13</sup> The combination of simple low-cost fabrication methods, including spin-coating, inkjet printing, and spray-coating, and the availability of diverse substrate materials, such as glass or flexible plastic, represent key advantages of organic semicon-

\* To whom correspondence should be addressed. E-mail: frances.ligler@nrl.navy.mil.

<sup>†</sup> Naval Research Laboratory.

<sup>‡</sup> NanoIdent Technologies AG.

(1) Chin, C. D.; Linder, V.; Sia, S. K. *Lab Chip* 2007, 7, 41–57.

(2) Whitesides, G. M. *Nature (London)* 2006, 442, 368–373.

(3) Kuswandi, B.; Nuriman; Huskens, J.; Verboom, W. *Anal. Chim. Acta* 2007, 601, 141–155.

(4) Hofmann, O.; Miller, P.; Sullivan, P.; Jones, T. S.; deMello, J. C.; Bradley, D. D. C.; deMello, A. J. *Sens. Actuators, B* 2005, 106, 878–884.

(5) Vo-Dinh, T.; Alarie, J. P.; Isola, N.; Landis, D.; Wintenberg, A. L.; Ericson, M. N. *Anal. Chem.* 1999, 71, 358–363.

(6) Golden, J. P.; Ligler, F. S. *Biosens. Bioelectron.* 2002, 17, 719–725.

(7) Jorgensen, A. M.; Mogensen, K. B.; Kutter, J. P.; Geschke, O. *Sens. Actuators, B* 2003, 90, 15–21.

(8) Edel, J. B.; Beard, N. P.; Hofmann, O.; DeMello, J. C.; Bradley, D. D. C.; DeMello, A. J. *Lab Chip* 2004, 4, 136–140.

(9) Schinlinsky, P.; Waldauf, C.; Hauch, J.; Brabec, C. J. *Thin Solid Films* 2004, 451, 105–108.

(10) Ramuz, M.; Burgi, L.; Winnewisser, C.; Seitz, P. *Org. Electron.* 2008, 9, 369–376.

(11) Hofmann, O.; Wang, X.; Huang, J.; Atkins, S.; Sullivan, P.; Bradley, D. D. C.; deMello, A. J.; deMello, J. C. *Proc. SPIE* 2005, 5938, 1–7.

(12) Peumans, P.; Bulovic, V.; Forrest, S. R. *Appl. Phys. Lett.* 2000, 76, 3855–3857.

(13) Yu, G.; Zhang, C.; Heeger, A. J. *Appl. Phys. Lett.* 1994, 64, 1540–1542.

Report Documentation Page				Form Approved OMB No. 0704-0188	
Public reporting burden for the collection of information is estimated to average 1 hour per response, including the time for reviewing instructions, searching existing data sources, gathering and maintaining the data needed, and completing and reviewing the collection of information. Send comments regarding this burden estimate or any other aspect of this collection of information, including suggestions for reducing this burden, to Washington Headquarters Services, Directorate for Information Operations and Reports, 1215 Jefferson Davis Highway, Suite 1204, Arlington VA 22202-4302. Respondents should be aware that notwithstanding any other provision of law, no person shall be subject to a penalty for failing to comply with a collection of information if it does not display a currently valid OMB control number.					
1. REPORT DATE <b>2009</b>		2. REPORT TYPE		3. DATES COVERED <b>00-00-2009 to 00-00-2009</b>	
4. TITLE AND SUBTITLE <b>Organic Photodiodes for Biosensor Miniaturization</b>				5a. CONTRACT NUMBER	
				5b. GRANT NUMBER	
				5c. PROGRAM ELEMENT NUMBER	
6. AUTHOR(S)				5d. PROJECT NUMBER	
				5e. TASK NUMBER	
				5f. WORK UNIT NUMBER	
7. PERFORMING ORGANIZATION NAME(S) AND ADDRESS(ES) <b>Naval Research Laboratory, 4555 Overlook Avenue SW,, Washington, DC, 20375</b>				8. PERFORMING ORGANIZATION REPORT NUMBER	
9. SPONSORING/MONITORING AGENCY NAME(S) AND ADDRESS(ES)				10. SPONSOR/MONITOR'S ACRONYM(S)	
				11. SPONSOR/MONITOR'S REPORT NUMBER(S)	
12. DISTRIBUTION/AVAILABILITY STATEMENT <b>Approved for public release; distribution unlimited</b>					
13. SUPPLEMENTARY NOTES					
14. ABSTRACT					
15. SUBJECT TERMS					
16. SECURITY CLASSIFICATION OF:			17. LIMITATION OF ABSTRACT <b>Same as Report (SAR)</b>	18. NUMBER OF PAGES <b>7</b>	19a. NAME OF RESPONSIBLE PERSON
a. REPORT <b>unclassified</b>	b. ABSTRACT <b>unclassified</b>	c. THIS PAGE <b>unclassified</b>			

ductor detectors over their silicon-based counterparts. In addition, from an instrumentation requirement perspective, expensive cameras or high precision scanning stages, along with the systems needed to align the sensing surface and detector are no longer necessary, as the readout can be fully integrated with the sensor surface. Also, the short optical pathway associated with integrated OPDs minimizes the loss of optical signal and allows for highly sensitive detection measurements, even without collection lenses.

Efficient OPD photodetection is dependent upon on high photon collection efficiency combined with photosensors that have low dark currents and high quantum efficiency.<sup>9,13</sup> Current technology allows OPDs to be fabricated with quantum efficiencies of over 50% and dark current densities of <10 nA/cm<sup>2</sup> in the visible spectrum.<sup>10,14,15</sup> Sensors for touch and luminescence have been reported that incorporate organic photodiodes. Bürgi et al. (2005) reported a proximity sensor based on the integration of polymer LEDs and OPDs on a single substrate.<sup>16</sup> DeMello's group reported the use of OPDs as detectors for chemiluminescence; the chemiluminescence sensors could detect hydrogen peroxide in solution to 10  $\mu$ M with a linearity over three decades.<sup>4,11,17</sup>

Using a layer-by-layer printing process, we have prepared OPDs on one side of a microscope slide. For protection against oxygen and moisture, the sensitive pixel areas were encapsulated with a customized oxygen barrier foil. Previous studies showed that these OPDs could efficiently detect light for a distance of about 2 mm with a photoresponse capability spanning 6 orders of magnitude.<sup>18</sup> The signal detection limit was determined to be 450 fW/mm<sup>2</sup>. Quantum efficiencies at 532 nm, shunt resistance, and noise-equivalent power were comparable to silicon photodiodes, but the risetime was slower ( $\mu$ s for OPDs compared to ns for silicon photodiodes). However, for most biosensor application, microsecond response times are quite sufficient. These OPDs were able to detect the signal from horseradish peroxidase spotted on to the surface above them at concentrations as low as  $2 \times 10^8$  molecules/mm<sup>2</sup>.

Here we report the first application of organic photodiodes in a biosensor for detection of a biological target. We have fabricated OPDs on glass slides with an active area of  $4 \times 4$  mm and a quantum efficiency of 50–60% at 532 nm. An accompanying portable hand-held device that can be plugged into any computer was developed for readout of the OPD signal. The combination of compact hand-held electronics and organic photodiodes detected photocurrents of less than 1 pW/mm<sup>2</sup>. Using this system, sandwich immunoassays were performed on the OPD substrate for detection of Staphylococcal enterotoxin B (SEB). Results demonstrated detection sensitivities better than typical ELISA-based laboratory tests and comparable to sensitivities reported using biosensors with CCD- and PMT-based detection.

## EXPERIMENTAL SECTION

**Organic Photodiode Sensors.** Organic photodiode sensors were produced in a dedicated fabrication facility. First, the structure of the transparent bottom ITO-electrode on 0.7 mm thick glass sheets was generated in a standard wet-chemistry etching procedure. Next, a  $\sim$ 100 nm diameter hole-conduction layer of poly(3,4-ethylene-dioxythiophene):polystyrene sulfonate (PEDOT:PSS) was deposited onto the transparent electrode using ink-jet printing. The PEDOT:PSS was then annealed to remove trapped water vapor. Ink jetting and spin coating, respectively, were used to deposit active layers of poly(3-hexylthiophene) (P3HT) and 1-(3-methoxycarbonyl)-propyl-1-phenyl-(6,6)C61 (PCBM) over the PEDOT:PSS. The layers were then annealed to improve the blend film morphology. The top electrode layer was formed by vacuum deposition of  $\sim$ 100 nm of aluminum through a shadow mask. The  $4 \times 4$  mm active area of the pixel was defined by the spatial overlap of the ITO and Al electrode. After annealing, the photodiodes were encapsulated with a customized single-sided pressure-sensitive oxygen barrier foil. Finally, in a semiautomated dicing process, individual slides were fabricated to  $25.5 \times 75.5$  mm, the size of standard microscope slides. Following fabrication, the photodiodes were characterized optoelectronically using an in-house testing platform. Using this platform, the sensitivity, quantum efficiency, dark current, linear range, and transient behavior of the sensors were determined. Sensors were labeled with a barcode for future identification.

**OPD Controller.** Electronics were optimized for the readout of the organic photodiodes at small reverse-bias voltages (0 to 100 mV) to achieve very low dark currents (low pA range) and low noise ( $\sim$  10 fA), resulting in very low limits of detection. For power-supply and communication with a laptop, PC, or PDA, the controller was equipped with a USB-mini standard interface. A simple press and release mechanism in the controller allowed for placement of the sensor using elastomeric connector pads.

A software package was developed in LabView (National Instruments, developer Suite 8.5). Included in the package was an installer for Microsoft Windows XP, drivers, and configuration files for data readout and analysis. The user interface allowed for sensor barcode entry which automatically calibrated the controller with the sensor data acquired during initial testing. In addition, the software was designed to allow the operator to display the photocurrent in real time and customize the controller settings such as signal integration time and sensitivity level to match the requirements of the assay.

**Fabrication of PDMS Reservoirs.** Poly(methylmethacrylate) (PMMA) molds to be used as templates for poly(dimethylsiloxane) (PDMS) reservoirs were milled using a numerically controlled milling machine (Techno Isel). PDMS reservoirs were made from NuSil MED-4011 silicone elastomer (NuSil Silicone Technology) as described in detail by Golden et al.<sup>19</sup> with the exception that reservoirs in the current work contained a 1 mL capacity single chamber versus 12- or 15-well reservoirs as utilized in the previous work.

**Optimization of Enzyme Concentration.** The horseradish peroxidase (HRP) concentration was optimized using both coverslips and on-slide OPD immunoassays. Coverslips and slides

(14) Inganas, O.; Roman, L. S.; Zhang, F. L.; Johansson, D. M.; Andersson, M. R.; Hummelen, J. C. *Synth. Met.* **2001**, *121*, 1525–1528.

(15) Granstrom, M.; Petritsch, K.; Arias, A. C.; Friend, R. H. *Synth. Met.* **1999**, *102*, 957–958.

(16) Bürgi, L.; Pfeiffer, R.; Mucklich, M.; Metzler, P.; Kiy, M.; Winnewisser, C. In *Building European OLED Infrastructure*, 1st ed.; SPIE: Cambridge, U.K., 2005; Vol. 5961, p 596104-34.

(17) Wang, X.; Hofmann, O.; Das, R.; Barrett, E. M.; deMello, A. J.; deMello, J. C.; Bradley, D. D. C. *Lab Chip* **2007**, *7*, 58–63.

(18) Pieler, R.; Fureder, E.; Sonleitner, M. In *Electro-Optical Remote Sensing, Detection, and Photonic Technologies and Their Applications*, 1st ed.; SPIE: Florence, Italy, 2007; Vol. 6739, p 673919-8.

(19) Golden, J.; Shriver-Lake, L.; Sapsford, K.; Ligler, F. *Methods* **2005**, *37*, 65–72.

(with OPDs on opposite side) were cleaned with a 10% (w/v) potassium hydroxide (KOH)/methanol (MeOH) solution for 1 h, rinsed with dH<sub>2</sub>O and dried using an air stream. Coverslips and slides were then treated with a 2% 3-aminopropyltrimethoxysilane (Gelest) solution in MeOH under nitrogen for 1 h, rinsed with MeOH, then dried using an air stream. Finally, coverslips and slides were coated with 50 mM EZ link N-hydroxysuccinimide-biotin (Pierce Scientific) for 1 h, rinsed with dH<sub>2</sub>O and stored in PBS at 4 °C until required.

For optimization experiments, coverslips and slides were blocked with Enhanced Chemiluminescence (ECL) Advance blocking agent (GE Healthcare) for 30 min and rinsed with phosphate buffered saline, 0.1% Tween 20, 1 mg/mL bovine serum albumin, pH 7.4 (PBSTB). Coverslips and slides were then treated with a series of NeutrAvidin (NA)-HRP (Thermo Scientific) dilutions ranging from 1:100 to 1:10,000 for 1 h, rinsed with PBSTB, dH<sub>2</sub>O, and dried using an air stream. Coverslips and slides were then placed in the controller, and measurements were taken as described in the immunoassay sections below.

**Biotinylated Antibody Preparation.** A monoclonal antibody against SEB (clone 2B, BioVeris) was labeled with EZ-link NHS-LC-Biotin at a 5:1 molar ratio according to the manufacturer's instructions (Pierce Scientific). The labeled antibodies were separated from free biotin on a BioGel P-10 column (Bio-Rad) equilibrated with PBS. Absorbance at 280 nm was used to determine antibody concentration.

**Immunoassays on Coverslips.** Coverslips (22 × 22 mm, Daigger) were prepared as described by Golden et al.,<sup>19</sup> with the exception that all steps were performed in mini-Coplin jars up to the point of HRP substrate addition. Briefly, coverslips were cleaned with a 10% (w/v) potassium hydroxide (KOH)/methanol (MeOH) solution, rinsed with dH<sub>2</sub>O, and dried using an air stream. Coverslips were then treated with a 2% 3-mercaptopropyltrimethoxysilane (Fluka Chemical) solution in MeOH. Slips were rinsed with MeOH and incubated with the heterobifunctional cross-linker *N*-[ $\gamma$ -maleimidobutyryloxy]succinimide ester, 1 mM (Fluka Chemical) in absolute ethanol. Finally coverslips were rinsed with dH<sub>2</sub>O and incubated with 30  $\mu$ g/mL NeutrAvidin (Pierce Scientific) in PBS at 4 °C overnight. After rinsing with PBS, the coverslips were kept at 4 °C until required.

For assays, NeutrAvidin-coated coverslips were incubated with 10  $\mu$ g/mL biotinylated  $\alpha$ -SEB antibody (clone 2B, BioVeris) for 2 h at room temperature and then rinsed with PBS. Coverslips were blocked with ECL Advance blocking agent for 30 min and rinsed with PBSTB. Coverslips were then incubated with the appropriate concentration of SEB (Toxin Technology) for 10 min, rinsed with PBSTB, and incubated with a 1:400 dilution of horseradish peroxidase-conjugated  $\alpha$ -SEB antibody ( $\alpha$ -SEB-HRP) (Toxin Technology). Coverslips were rinsed with PBSTB, dried using an air stream, and attached to the unmodified sensor surface opposing the photodiode using glycerol as a refractive index matching solution. Following insertion into the OPD controller, baseline measurements were taken. Equal volumes of Lumingen TMA-6 Solutions A and B (substrate) were mixed according to the manufacturer's instructions (Echemiluminescence Advance Western Blotting Detection Kit; GE Healthcare) and 200  $\mu$ L was added directly to the coverslip through a port in the cover of the controller. Measurements were then taken for at least 200 s post-

substrate addition. All readings utilized controller settings of medium sensitivity and a 500 ms integration time. For the purposes of generating a standard curve, the normalized signal corresponded to the peak signal taken within 60 s post-substrate addition minus baseline, defined as the stable signal interval obtained just prior to addition of the substrate.

**Immunoassays on OPD Sensors.** Immobilization and assay steps were identical between experiments utilizing coverslips and OPD slides with the exception that PDMS reservoirs rather than mini-Coplin jars were used for preparation of the slides. PDMS reservoirs (1 mL capacity) were attached to the slides using milled PMMA chucks to confine reagents to the surface opposite, and directly superior to, the photodiode. Following incubation with a 1:700 dilution of  $\alpha$ -SEB-HRP, slides were rinsed with PBSTB, dried using an air stream, fitted with an adhesive opaque microfluidic flow chamber (Ibidi Integrated Biodiagnostics), and inserted into the controller. Substrate (200  $\mu$ L) was then added through the port in the lid of the reader, and the resulting signal was taken from 60–70 s (20 data points) post-substrate addition. Normalized signal corresponded to the absolute signal minus baseline. The baseline was defined as the stable 10 s (20 data points) signal interval obtained just prior to addition of the substrate.

## RESULTS AND DISCUSSION

The optoelectronic detection system was composed of two principal components: a disposable biosensing element and a hand-held controller (Figure 1, panels A and B). The disposable sensor element had the dimensions of a traditional glass microscope slide (25.5 mm × 75.5 mm) and contained a printed organic photodiode with associated electrodes for transmission of the electronic signal to the controller. A USB interface connected the controller to a PC computer installed with the integration software. OPDs are inexpensive, and the NanoIdent fabrication capabilities enabled batch production of 500–700 sensors per week with various predetermined photodiode geometries. The OPDs were located on the opposite side of a glass surface that could be pre-coated with specific antibodies of interest or generic capture molecules for future use.

The hand-held controller measured 17.1 cm × 7.8 cm × 3.8 cm and weighed less than 215 g. It consisted of an internal alignment chamber that utilized a cantilever to hold the sensing slide stationary and a hard plastic outer casing that shielded the internal controller components from light and dust. Because of the nature of the readout method, shielding from ambient light was extremely important. A small 1.6 mm port in the lid of the casing was used to deliver substrate reagents during the assay. In addition, an opaque microfluidic chamber was attached to the sensing slide prior to reading. The integration software proved to be versatile and user-friendly, having options for the display type, user entry assay description, signal integration time, and desired sensitivity. Assay data and descriptions were stored as txt files and analyzed in a generic spreadsheet such as Microsoft Excel.

To determine the capabilities of the OPD LOC system, the performance of the organic photodiodes was investigated using a NanoIdent in-house testing system (Table 1). Following characterization of the OPDs, the detection potential of the system for a biological agent was investigated. For these experiments, SEB was selected as the target. We have previously demonstrated detection of SEB using the same anti-SEB antibody in three other



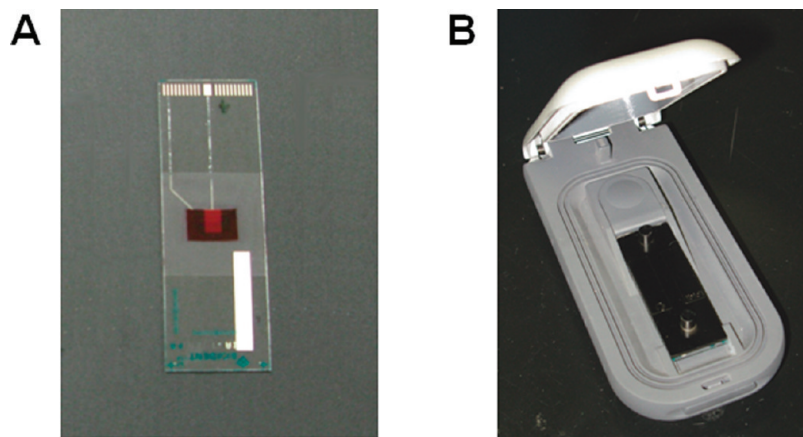


**Figure 1.** Components of the OPD biosensor. (A) Glass sensor slide containing a centrally located printed OPD and the associated electrodes. (B) The hand-held controller that can be connected to any computer using a USB interface.

**Table 1. OPD Sensor Performance Characteristics**

parameter	comment	units	value
sensitivity (S)	$\lambda = 532 \text{ nm}$	A/W	0.25
photocurrent drift ( $\Delta I_p$ , 5 min)	$((I_{p, \text{Max}} - I_{p, \text{Min}})) / (\text{mean}(I_p))$ within 5 min	%	0.05
dark-current-density ( $i_d$ )	@ 0–100mV reverse bias voltage	A/mm <sup>2</sup>	$1-10 \times 10^{-12}$
dark-current-density noise ( $n(i_d)$ )	@ 0–100mV reverse bias voltage	A/mm <sup>2</sup>	$10-150 \times 10^{-15}$
estimated Limit of Detection (LOD)	$(3n(i_d)) / (S)$	W/mm <sup>2</sup>	$10^{-13}-10^{-12}$

biosensors, allowing for the direct comparison to data obtained using the OPD biosensor to that produced using commercially available systems. Because the electronic components of the OPD sensor (photodiode and electrodes) are on the bottom surface of the slide, all attachment and assay chemistry steps are performed on the opposite surface. After toxin capture and incubation with the HRP-conjugated tracer antibody, the chemiluminescent signal generated upon the addition of substrate is detected by the photodiode and relayed by the controller to the computer.

During sensor preparation, reasonable care was necessary to minimize exposure of the sensor electronic components to damaging solvents or reagents. Initially, we utilized  $22 \times 22 \text{ mm}$  coverslips as a surrogate surface on which all the chemistry steps were performed. This coverslip approach not only avoided exposing the OPD to solvent, but also permitted the use of a single OPD with multiple coverslips. This reutilization reduced labor and expense at the initial testing stage, permitting batch preparation of antibody coatings, and eliminated potential variation in results due to any sensitivity differences among the OPDs. Coverslips were used only during this initial optimization stage and were not intended for use in the final version of the assay.

Prior to running SEB detection assays on the coverslips, the HRP concentration was optimized. Coverslips coated with immobilized biotin were exposed to a broad range of NeutrAvidin (NA)-HRP concentrations ranging from 1:100–1:10,000. These dilutions corresponded to HRP concentrations ranging from  $10 \mu\text{g/mL}$  to  $100 \text{ ng/mL}$  and an activity of  $1.77 \text{ U/mL}$  to  $0.0177 \text{ U/mL}$ , respectively. From these experiments, a 1:400 dilution was found to be optimal in terms of maximizing sensitivity and minimizing the background of the assay using coverslips (data not shown). Detection of a colorimetric product following the addition of 3,3', 5,5'-tetramethylbenzidine (TMB) substrate to the

coverslips verified the HRP activity in the titration experiments (data not shown).

SEB sandwich immunoassays were then performed. Coverslips coated with biotinylated  $\alpha$ -SEB capture antibody were first exposed to various concentrations of SEB, ranging from  $0 \text{ ng/mL}$  to  $10 \text{ ng/mL}$ , and then to  $\alpha$ -SEB-HRP tracer antibody at a 1:400 dilution. Following addition of the  $\alpha$ -SEB-HRP antibody, each coverslip was mounted to the sensor surface opposite the OPD using a refractive index matching solution (glycerol). The sensor/coverslip combination was then inserted into the controller, and baseline readings were taken. Baseline was defined as the mean signal intensity prior to the addition of substrate. Following substrate addition, there was a characteristic brief spike in signal intensity followed by a lower steady signal persisting for at least 200 s (Figure 2). From these experiments, a standard curve was generated, and the detection limit for SEB was determined to be approximately  $0.1 \text{ ng/mL}$  (Figure 3). Values for the standard curve were obtained by subtracting baseline signal prior to substrate addition from the steady-state signal obtained within 60 s after the addition of substrate.

To improve the detection limit and to increase signal levels beyond those obtained using the coverslip approach, antibodies were immobilized directly on the slide. We refer to this method as the on-slide approach. Immobilization procedures were restricted to the surface opposite the OPD to avoid exposing the OPD to potentially damaging solvents. To accomplish this, a single-use poly(dimethylsiloxane) (PDMS) elastomer reservoir was designed that could be placed over the sensing surface directly above the OPD. The PDMS reservoir was held in place on the slide using a PMMA chuck and contained the fluids and reagents throughout the assay (Figure 4). As with the coverslip experiments, the antibody-HRP concentration was optimized. In

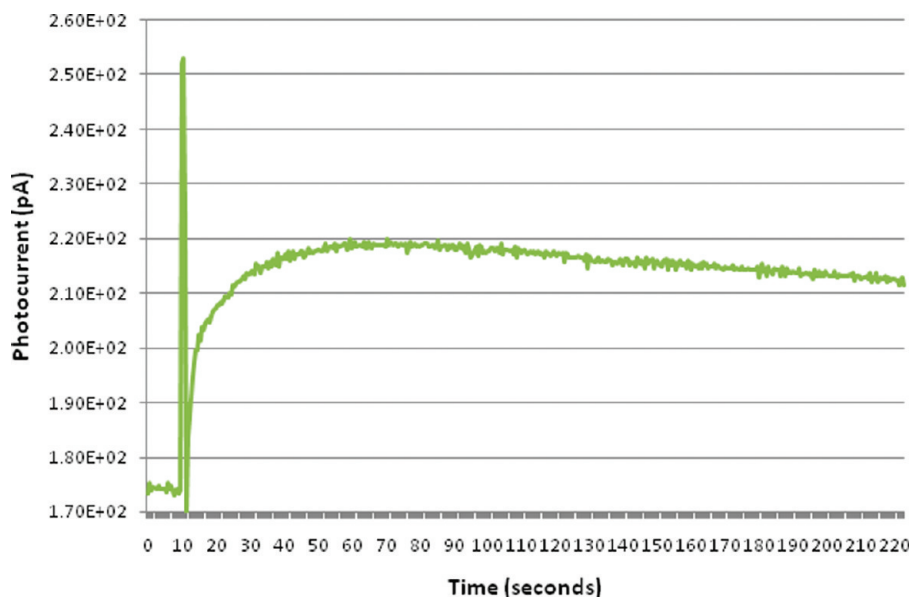


**Figure 2.** Chemiluminescent reaction on coverslips generates a detectable signal. Coverslips were coated with  $\alpha$ -SEB capture antibody, exposed to varying concentrations of SEB ranging from 0 ng/mL to 10 ng/mL, and followed by HRP-coupled  $\alpha$ -SEB antibody at a 1:400 dilution. Substrate was added  $\sim 20$  s into the reading. Plot is representative of three experiments using an SEB concentration of 5 ng/mL.

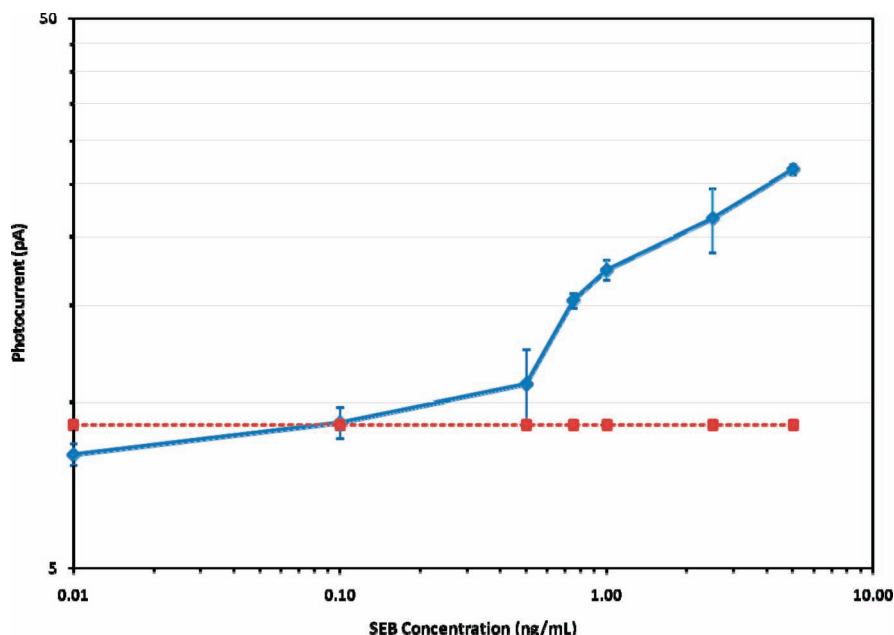


**Figure 3.** Dose–response curve for SEB detection on coverslips. Coverslips were coated with NeutrAvidin, then biotinylated  $\alpha$ -SEB capture antibody was immobilized on the surface. Coverslips were exposed to varying concentrations of SEB for 10 min followed by  $\alpha$ -SEB-HRP antibody at a 1:400 dilution. Coverslips were mounted to the sensor, inserted into the reader, and readings were taken as described in the Experimental Section. Each data point represents the mean of 3–5 independent measurements. The horizontal dashed line represents the limit of detection (LOD) as defined as the equivalent of  $3\times$  the standard deviation of the signal obtained with 0 ng/mL SEB.

this case, a 1:700 dilution was found to be optimal for assays in which chemistry was performed directly on the OPD slide (data not shown).

To detect SEB, the OPD slides were coated with biotinylated  $\alpha$ -SEB antibodies, exposed to various concentrations of SEB (0–50 ng/mL), and incubated with  $\alpha$ -SEB-HRP tracer antibodies. Sensors were then fitted with an opaque microfluidic chamber and placed into the OPD controller for reading (Figure 1B and Figure 4). For the purposes of generating the standard curve, a 10 s time interval from 60 to 70 s after the addition of the substrate was used, as the signal was stable at this time period. This 10 s interval

included 20 individual data points using a 500 msec integration time. To obtain the adjusted signal, the baseline signal was subtracted from the raw 60 s signal. A representative signal plot for 5 ng/mL SEB is shown in Figure 5. The dose–response curve for SEB is shown in Figure 6. The limit of detection, designated as the lowest concentration of SEB tested that was greater than the mean of the no-SEB samples plus 3 SD, was approximately 0.5 ng/mL.

Comparison of the coverslip and on-slide approaches revealed several differences between the two procedural variants. The photocurrents generated in the on-slide assays were over 5-fold

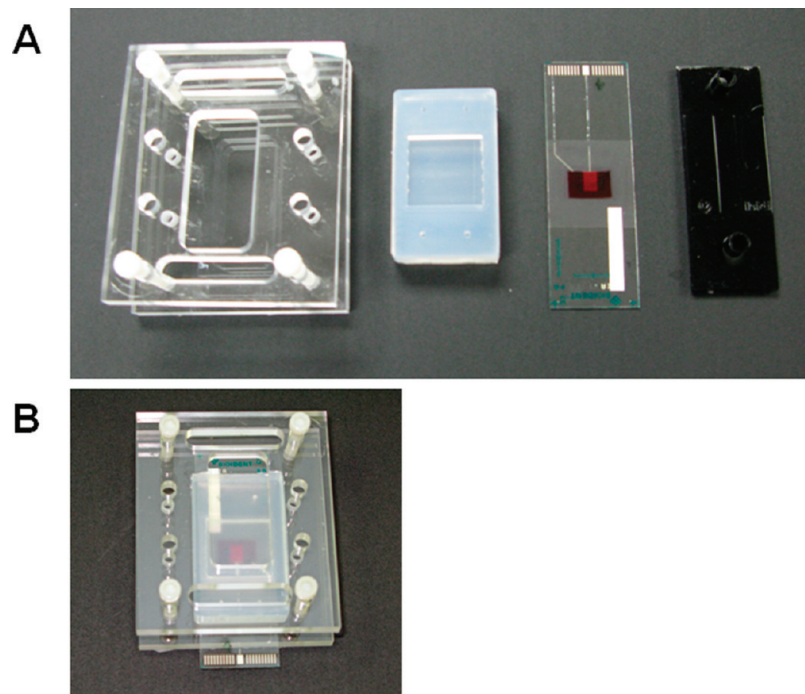


**Figure 4.** Accessories for SS assays. (A) From left to right: Poly(methylmethacrylate) (PMMA) holder, poly(dimethylsiloxane) (PDMS) reservoir, sensor slide containing a centrally located OPD and microfluidic channel. (B) The PMMA holder sandwiches the sensor to the PDMS reservoir to confine the immobilization and assay chemistry to the surface of the sensor opposite the OPD. Screws are hand-tightened to create a watertight seal.

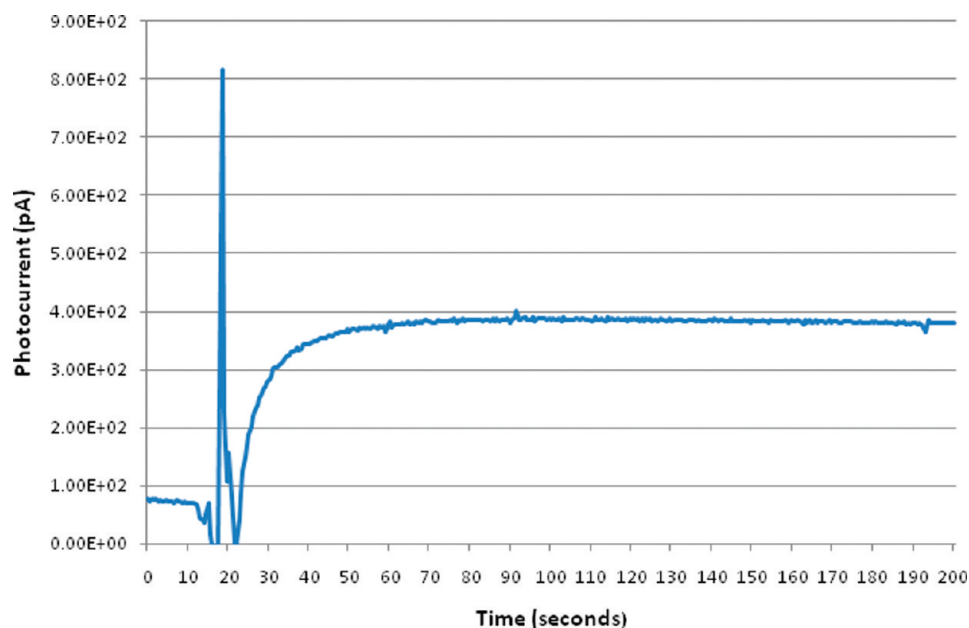


**Figure 5.** Chemiluminescent reaction directly on the sensor generates a detectable signal. Slides were coated with  $\alpha$ -SEB capture antibody, exposed to varying concentrations of SEB ranging from 0 ng/mL to 50 ng/mL, and incubated with an HRP-coupled  $\alpha$ -SEB antibody at a 1:700 dilution. Substrate was added ~20 s into the reading. Plot is representative of five experiments using an SEB concentration of 5 ng/mL.

greater than those produced in the coverslip assays as SEB concentrations rose over 0.1 ng/mL. These enhanced signals occurred despite a larger  $\alpha$ -SEB-HRP antibody dilution in the on-slide assays (1:700 vs 1:400), suggesting that on-slide assays provided the more efficient method for measuring the chemiluminescent signal. The increased signal for the on-slide approach is likely due to the shorter path distance between the chemiluminescent reaction and the OPDs. Although one might expect

this enhanced photocurrent to increase the sensitivity, this was not the case. While higher intensity signals were observed in on-slide assays, the standard deviation of the measurements was also larger. This in turn affected our LOD. Experiments with coverslips may have demonstrated decreased standard deviations because (1) a single OPD was used for multiple readings and (2) the coverslips were prepared in batches. The former minimizes individual sensor variation while the latter ensures preparation



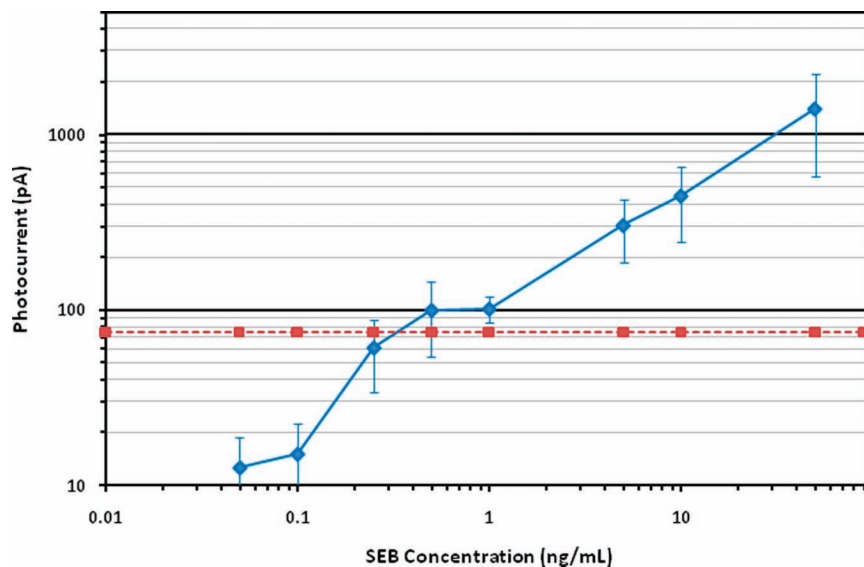


**Figure 6.** Dose–response curve for SEB detection on sensors. Sensors were coated with NeutrAvidin, and biotinylated  $\alpha$ -SEB capture antibody was immobilized on the surface. The sensing surfaces were exposed to varying concentrations of SEB for 10 min, followed by HRP-coupled  $\alpha$ -SEB antibody at a 1:700 dilution. Slides were fitted with opaque microfluidic chambers, inserted into the reader, and read as previously described. Each data point represents the mean of 3–5 independent measurements. The horizontal dashed line represents the limit of detection (LOD) as defined as the equivalent of  $3\times$  the standard deviation of the signal obtained with 0 ng/mL SEB.

homogeneity. If the deviation can be reduced for the on-slide assays, this approach has the potential to detect even lower concentrations of the target analyte. Despite a similar LOD for both approaches, the on-slide assay is more desirable in that it offers the possibility of quantitation of SEB from an unknown sample. The signal range and slope of the standard curve for the on-slide OPD sensor experiments was larger for the SEB concentrations tested (1 to 50 ng/mL) and supports the potential for quantitation within that range.

In terms of biosensor performance, the OPD system is comparable to other antibody-based systems using the same reagents. It yields results similar to the PMT-based RAPTOR fiber optic biosensor (Research International) in terms of both time and sensitivity, as both systems are able to detect  $\geq 0.5$  ng/mL SEB in less than 30 min.<sup>20</sup> In comparing the OPD system to the CCD-based Array Biosensor, the latter was able to achieve slightly lower detection of SEB using the same 30 min detection period (0.1 ng/mL vs 0.5 ng/mL, respectively).<sup>21,22</sup> However, an important consideration in evaluating these results is the true portability of the OPD system. While the RAPTOR and Array Biosensor are described as portable, they both are substantially larger, heavier, and costlier than the OPD controller and thus are less suitable for point-of-use applications. While platforms such as the Luminex flow cytometer are able to detect lower levels of SEB (50–100 pg/mL), such systems require much longer incubation times<sup>23</sup> (up to 2 h) and are not portable. In the event that lower detection limits are required, sensitivity may also be enhanced by adjusting the controller settings used during data acquisition. An integration time of 500 msec and a medium sensitivity setting were used for

both coverslip and on-slide assays. Switching the controller to a longer integration time and/or using a high sensitivity setting may decrease the LOD. In addition, the incubation protocol could be lengthened, as increases in incubation time such as those used for the Luminex have been shown to improve sensitivity. However, because point-of-care diagnostics and many point-of-use assays need to be rapid, lengthening the assay time may not be advantageous.

## CONCLUSION

In summary, we have demonstrated the use of organic photodiodes for highly sensitive detection of a toxin using a hand-held biosensor. The OPD system described herein is rapid, portable, and robust. The OPDs are inexpensive to manufacture, and the instrumentation is hand-held, versatile, and extremely user-friendly, only requiring a laptop for data acquisition and analysis. While the disposable component utilized in these experiments only contained a single photodiode, the technology can be converted into a multiplex format by printing several photodiodes on a single substrate.<sup>18</sup> Such an array configuration could be used to test multiple samples for several targets simultaneously, expanding the capabilities and utility of this detection system.

## ACKNOWLEDGMENT

This work was supported by Defense Advanced Research Project Agency (DARPA) seed grant 11F000113. The views expressed here are those of the authors and do not represent those of the U.S. Navy, the U.S. Department of Defense (DOD), or the U.S. Government.

Received for review December 23, 2008. Accepted March 16, 2009.

AC8027323

(20) Jung, C. C.; Saaski, E. W.; McCrae, D. A.; Lingerfelt, B. M.; Anderson, G. P. *IEEE Sens. J.* **2003**, *3*, 352–360.

(21) Shriver-Lake, L. C.; Shubin, Y. S.; Ligler, F. S. *J. Food Prot.* **2003**, *66*, 1851–1856.

(22) Sapsford, K. E.; Taitt, C. R.; Loo, N.; Ligler, F. S. *Appl. Environ. Microbiol.* **2005**, *71*, 5590–5592.

(23) Anderson, G. P.; Taitt, C. R. *Biosens. Bioelectron.* **2008**, *24*, 324–328.